静置し、各穴 300µl の PBS-Tween で 3 回洗浄して 3 の検体分注に供する。

3. 血清及び標準曲線用組換え可溶性 CD26 の添加

PBS-Tween20 で 20 倍に希釈した対象血清を 100µl ずつ 2 穴に分注する。標準曲線を作成するため、段階希釈（500, 250, 125, 62.5, 31.3, 15.6, 7.8, 3.9, 1.95, 0.98, 0.49, 0 ng/ml）した組換え可溶性 CD26 標準試薬（R&D systems, Inc.）を 100µl ずつ 2 穴に分注する。プレートを密封し、4℃で一晩静置する。

4. 可溶性 CD26 の測定

上記 3 のプレートを各穴 300µl の PBS-Tween で 3 回洗浄後、0.5µg/ml の検出抗体（ビオチン化 CD26 単クローン抗体 9C11 あるいは 1F7）を各穴 100µl ずつ分注し、室温で 2 時間静置する。300µl の PBS-Tween で 3 回洗浄後、1 万倍希釈した ExtrAvidin-Alkaline Phosphatase 液を 100µl ずつ分注する。プレートを遮光して、室温で 1 時間静置する。300µl の PBS-Tween で 3 回洗浄後、PNPP を 100µl ずつ分注し、遮光して室温で 10 分間静置した後、2N-NaOH 溶液を 100µl ずつ分注して、発行反応を停止させる。プレートリーダーで吸光度を測定する（吸光度 405nm、レファレンス 655nm）。

【DPPIV 酵素活性の測定】

1. 捕捉抗体プレートの作成とブロッキング

上記 2)の 1 及び 2 と同様に捕捉抗体プレートを作成し、ブロッキングをする。

2. 血清及びポジティブコントロール用組換え可溶性 CD26 の添加

PBS-Tween で 10 倍に希釈した対象血清を 100µl ずつ 2 穴に分注する。ポジティブコントロールとして 500ng/ml に調整した組換え可溶性 CD26 標準試薬（R&D systems, Inc.）を 100µl ずつ 2 穴に分注する。プレートを密封し、4℃で一晩静置する。

3. DPPIV 酵素活性の測定

上記 2 のプレートを各穴 300µl の PBS-Tween で 3 回洗浄後、1mg/ml に調整した Gly-Pro-pNA を血清及びポジティブコントロールを添加したウェルに 150µl ずつ分注する。標準曲線を作成するため、段階希釈（1000, 500, 250, 125, 62.5, 31.3, 15.6, 7.8, 3.9, 0 µM）した pNA 溶液を 150µl ずつ分注する。直ちにプレートリーダーで吸光度を測定する（吸光度 405nm、レファレンス 655nm）。その後 75 分後まで（15 分毎に）吸光度を測定し、DPPIV 活性（µM/min）を計測する。

【比較対照とした既存の市販測定キット】

a) R & D Systems, Inc.

キット名：Quantikine Human CD26/DPPIV Immunoassay

捕捉抗体：抗ヒト CD26 単クローン抗体

検出抗体：HRP 標識・抗ヒト CD26 ポリクローナル抗体

発色：化学発光（吸光度 450nm）

b) Bender MedSystems GmbH（現 eBioscience）

キット名：Human sCD26 Platinum ELISA

捕捉抗体：抗ヒト CD26 単クローン抗体

検出抗体：ビオチン化抗ヒト CD26 単クローン抗体、Streptavidin-HRP

発色：化学発光（吸光度 450nm）

3) 健常人血清、本邦患者検体及びフランスの第 I 相臨床試験の患者血清について

健常人血清は研究室で働く研究者からインフォームドコンセントを得た後に採取した。

悪性中皮腫患者血清、胸水は1998年から2011年までに岡山労災病院及び山口宇部医療センターにおいて悪性中皮腫として診断・治療を受けた症例でインフォームドコンセントを得られた症例を用いている。

フランスでの第Ⅰ相臨床試験は平成21年1月からスタートして、第6コホートからなり、第1コホート0.1mg/kg、第2コホート0.4mg/kg、第3コホート1mg/kg、第4コホート2mg/kg、第5コホート4mg/kg、第6コホート6mg/kgで各コホートは3症例からなっている。第4コホートの途中までは2週間ごとの1ヶ月間月3回投与であった。その後第4コホートの途中から1ヶ月間毎週投与で月5回投与とプロトコールの変更を行っている。平成26年9月に第Ⅰ相臨床試験は終了した。合計34例の標準治療に抵抗性の悪性中皮腫患者(23例)腎癌(10例)、膀胱移行上皮癌（1例）であった。

（倫理面への配慮）

本研究の、特に臨床研究においては、文書により被験患者本人の同意を得た上で行うものとする。本研究にまつわる個人情報は厳重な管理のもと守秘義務を遵守する。また解析検討結果を公表する際には個人名の漏えい防止を徹底し、プライバシーの保護に努める。さらに個人に帰属する結果を個人に求められた場合には、その個人本人のもののみ伝達する旨である。

なお、フランスで実施されているヒト化CD26抗体投与の第Ⅰ相臨床試験における対象症例血清中の可溶性CD26及びDPPIV活性の測定及びコントロール症例の可溶性CD26及びDPPIV酵素活性の測定については順天堂大学の倫理審査委員会の審査にて承認されている（順天医倫第2012076及び2012087)。検体の使用は患者の同意が得られているかあるいは岡山労災病院、山口宇部医療センターの臨床研究審査委員会で承認を得て研究内容について院内掲示などで周知を図った。

試料を匿名化することで個人のプライバシーが漏れることのないように配慮した。

C. 研究結果

1) フランスの第Ⅰ相臨床試験の患者血清中の可溶性CD26及びDPPIV酵素活性値

フランスの第Ⅰ相臨床試験患者検体は第4コホート途中までの1ヶ月隔週投与例ではヒト化CD26抗体投与前、投与直後、2日後、15日後投与前、投与直後の血清、第4コホート途中以後はヒト化CD26抗体は1ヶ月毎週投与となったため、ヒト化CD26抗体投与前、投与直後、2日後、15日後投与前、投与直後、29日後投与前、投与直後の血清からなり、新しいELISA法にて可溶性CD26及びDPPIV値を測定した。図1にヒト化CD26抗体の血清中濃度、図2に可溶性CD26の血清中濃度を示した。ヒト化CD26抗体はコホートが上がり、投与濃度が増加するにつれ、血中濃度も上昇していた。それに対応して可溶性CD26濃度は低下していることが観察された。DPPIV酵素活性についても可溶性CD26濃度に並行して動き低下していくことが明らかとなった（図3)。

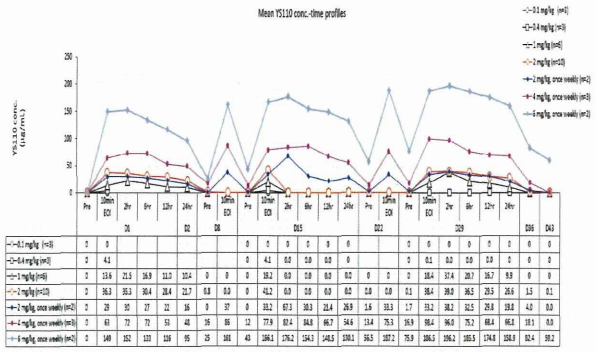

	Pre	10min D21	2hr	6hr	12hr	24hr	Pre	10min D8	Pre	10min D15	2hr	6hr	12hr	24hr	Pre	10min D21	Pre	10min D29	2hr	6hr	12hr	24hr	D36	D43
0.1 mg/kg (n=3)	0	0							0	0	0	0	0	0			0	0	0	0	0	0	0	0
0.4 mg/kg (n=3)	0	4.1							0	4.1	0.0	0.0	0.0	0			0	0.1	0.0	0.0	0.0	0	0	0
1 mg/kg (n=6)	0	13.6	21.5	16.9	11.0	10.4	0	0	0	16.2	0.0	0.0	0.0	0.0	0	0	0	18.4	37.4	20.7	16.7	9.9	0	0
2 mg/kg (n=10)	0	36.3	35.3	30.4	28.4	21.7	0.0	0.0	0	43.2	0.0	0.0	0.0	0.0	0.0	0.0	0.1	38.4	39.0	36.5	29.5	25.6	1.5	0.1
2 mg/kg, once a week (n=5)	0	28	30	27	22	16	9	37	0	33.2	67.1	30.3	21.4	26.9	1.6	33.3	1.7	33.2	38.2	32.5	29.8	19.0	4.0	0.0
4 mg/kg, once a week (n=3)	0	63	72	72	53	48	16	86	12	77.9	92.4	84.8	86.7	54.6	13.4	75.3	16.9	98.4	96.0	75.2	68.4	46.8	18.1	8.0
6 mg/kg, once a week (n=4)	0	149	152	133	116	95	25	168	43	166.1	176.2	154.3	148.5	130.1	56.5	187.2	75.9	186.5	196.2	165.5	174.8	158.3	82.4	50.2

図1 ヒト化CD26抗体の血清中濃度平均値の推移

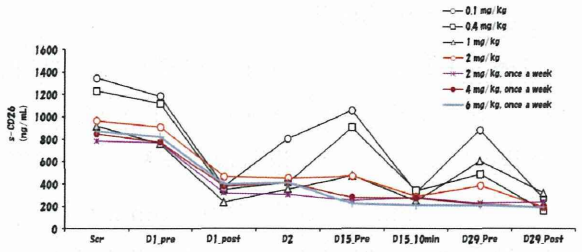

Dose	Scr	D1_pre	D1_post	D2	D15_Pre	D15_10min	D29_Pre	D29_Post
0.1 mg/kg	1344.0	1182.8	374.7	804.6	1054.0	325.7	882.0	265.5
0.4 mg/kg	1227.3	1116.4	348.3	416.6	902.6	338.7	487.1	160.3
1 mg/kg	914.1	758.4	236.2	352.7	470.7	247.3	605.1	318.1
2 mg/kg	960.2	905.0	462.1	451.2	467.9	283.1	381.7	189.9
2 mg/kg, once a week	779.0	766.8	315.3	302.6	250.7	275.7	227.3	234.8
4 mg/kg, once a week	843.6	769.9	374.6	409.1	277.8	270.3	215.8	191.2
6 mg/kg, once a week	869.7	818.2	396.6	410.1	221.1	207.9	209.1	189.7

図2 可溶性CD26の血清中平均濃度の推移

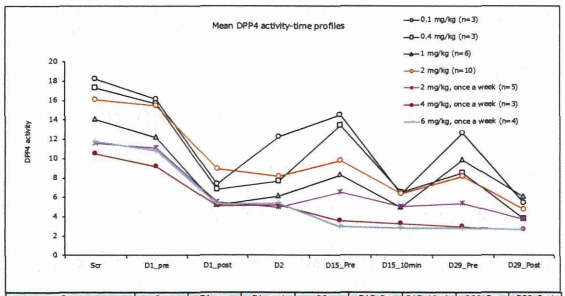

Dose	Scr	D1_pre	D1_post	D2	D15_Pre	D15_10min	D29_Pre	D29_Post
0.1 mg/kg (n=3)	18.2	16.1	7.3	12.2	14.5	6.3	12.6	5.4
0.4 mg/kg (n=3)	17.3	15.6	6.8	7.7	13.4	6.5	8.5	3.8
1 mg/kg (n=6)	14.0	12.2	5.2	6.1	8.3	4.9	9.8	6.0
2 mg/kg (n=10)	16.0	15.4	8.9	8.1	9.7	6.3	8.1	4.7
2 mg/kg, once a week (n=5)	11.5	11.1	5.5	4.9	6.5	5.0	5.4	3.7
4 mg/kg, once a week (n=3)	10.4	9.1	5.1	5.1	3.6	3.3	2.9	2.6
6 mg/kg, once a week (n=4)	11.7	10.8	5.3	5.4	3.0	2.8	2.8	2.6

図3 DPPIV酵素活性の血清中平均値の推移

2) 可溶性CD26 ELISAアッセイの性能試験と測定時間の簡便化

4種類の濃度の標準試料（5, 50, 150, 400ng/ml）を同時に8回測定することで同時再現性試験とした。表1に示したように変動係数（CV: Coefficient of variation）は10%以下と良好な結果を示した。次に4種類の濃度の標準試料（5, 50, 150, 400ng/ml）を5回繰り返して測定することで測定間再現性試験とした。表2に示したように変動係数（CV）が10%以下と良好な結果を示した。添加回収試験（Recovery）と直線性試験（Linearity）について添加回収試験（Recovery）はR&D system社のSpike and Recovery Test protocolに従って実地した（図4-1）。「試料」は健常成人血清を20倍希釈したものを使用。「添加あり」はrecombinant CD26（R&D#1180-SE）を最終濃度（50ng/ml）になるようにサンプルに添加した。図4-2に結果を示したがRecoveryは回収率 80～120%範囲内と良好な結果を示した。更にLinearityに関しても図4-2に結果を示したが直線性80~120%範囲内と良好な結果を示した。健常成人の血清検体の2週間までの4℃保存及び血清検体を10回まで凍結融解をくり回したが共に測定値の変化は認められなかった(データは未表示)。可溶性CD26定量ELISAアッセイの性能試験のまとめであるが性能試験の結果は良好であった。すなわち検量線、血清検体、捕捉抗体、検出抗体、希釈液等いずれも適切であると言える。最後に可溶性CD26濃度測定ELISAアッセイの短縮化の検討を行った。検体反応について従来法は一晩・静置・4℃で施行したが改訂版として2時間穏やかに振盪・室温で行い、健常成人血清11例について検討した。図5に示すように可溶性CD26測定は室温2時間の検体反応時間で従来法と同等の測定結果が得られた。以上より可溶性CD26測定に関して検体反応時間は一晩から2時間まで短縮可能である。

表1 同時再現性試験(Intra-assay):可溶性CD26定量アッセイ

標準試料	テスト1	テスト2	テスト3	テスト4	テスト5	テスト6	テスト7	テスト8	Mean	SD	CV(%)
5 ng/ml	5.33	4.96	4.62	4.85	5.06	5.04	4.89	5.06	4.98	0.20	4.09
50 ng/ml	48.50	50.98	49.30	51.20	51.47	51.60	51.69	53.58	51.04	1.55	3.04
150 ng/ml	142.47	155.10	153.40	152.34	159.13	156.74	155.68	162.53	154.67	5.89	3.81
400 ng/ml	388.49	399.37	398.86	417.97	392.53	405.96	390.13	418.48	401.60	11.83	2.95

4種類の濃度の標準試料(5, 50, 150, 400ng/ml)を
同時に8回測定することで同時再現性試験とした。

⇒ 変動係数CVが10%以下と良好な結果を示した。

表2 測定間再現性試験(Inter-assay):可溶性CD26定量アッセイ

標準試料	プレート1	プレート2	プレート3	プレート4	プレート5	Mean	SD	CV(%)
5 ng/ml	4.89	5.02	5.33	5.06	4.89	5.04	0.18	3.55
50 ng/ml	50.27	49.62	48.50	49.60	49.79	49.56	0.65	1.31
150 ng/ml	150.54	154.83	142.47	149.57	148.05	149.09	4.48	3.00
400 ng/ml	396.01	394.05	388.49	395.09	411.59	397.05	8.64	2.18

4種類の濃度の標準試料(5, 50, 150, 400ng/ml)を5回繰り返して
測定することで測定間再現性試験とした。

⇒ 変動係数CVが10%以下と良好な結果を示した。

1) アッセイの実施

キット付属のプロトコルに従い、Ⅲ・Ⅳで調整した試料を用いてアッセイを行います

プレートのウェル配置図

	1	2	3	4	5	6
A	スタンダード1		試料(添加あり)		コントロール(添加あり)	
B	スタンダード2		1:2 希釈の試料(添加あり)		1:2 希釈の試料(添加あり)	
C	スタンダード3		1:4 希釈の試料(添加あり)		1:4 希釈の試料(添加あり)	
D	スタンダード4		1:8 希釈の試料(添加あり)		1:8 希釈の試料(添加あり)	
E	スタンダード5		試料(添加なし)			
F	スタンダード6		1:2 希釈の試料(添加あり)			
G	スタンダード7		1:4 希釈の試料(添加あり)			
H	ブランク		1:8 希釈の試料(添加あり)			

2) 測定値の算出・解析

以下の計算式を使用して、測定値を算出し、解析を行います

1. 添加回収試験

$$\text{回収率(\% Recovery)} = \frac{\text{「試料(添加あり)」の測定値} - \text{「試料(添加なし)」の測定値}}{\text{添加した標準物質の量}} \times 100$$

2. 直線性試験

・「試料(添加あり)」の直線性を検討する場合、「試料(添加あり)」の測定値を「予測値とする」

・「試料(添加なし)」の直線性を検討する場合、「試料(添加なし)」の測定値を「予測値とする」

$$\text{1:2 希釈の回収率(\%)} = \frac{\text{1:2 希釈試料の測定値}}{\text{予測値} \div 2} \times 100$$

$$\text{1:4 希釈の回収率(\%)} = \frac{\text{1:4 希釈試料の測定値}}{\text{予測値} \div 4} \times 100$$

$$\text{1:8 希釈の回収率(\%)} = \frac{\text{1:8 希釈試料の測定値}}{\text{予測値} \div 8} \times 100$$

図4-1 添加回収試験(Recovery)と直線性試験(Linearity)の実施方法

添加回収試験(Recovery)

	試料(添加あり)	試料(添加なし)	回収率(%)
希釈なし	88.19	37.89	95.17
1/2希釈	43.13	20.39	98.44
1/4希釈	21.29	11.10	90.98
1/8希釈	11.72	4.83	109.19

⇒回収率80~120%範囲内と良好な結果を示した。

直線性試験(Linearity)

		直線性(%)
試料(添加あり)	1/2希釈	103.69
	1/4希釈	102.37
	1/8希釈	112.71

試料(添加なし)	1/2希釈	107.63
	1/4希釈	117.18
	1/8希釈	101.98

⇒直線性80~120%範囲内と良好な結果を示した。

図4-2 添加回収試験(Recovery)と直線性試験(Linearity)

添加回収試験(recovery)はR&D Systems社のSpike and Recovery Test Protocolに従って実施した。「試料」は健常成人血清(を20倍希釈したもの)を使用。
「添加あり」はrecombinant CD26を最終濃度50ng/mLになるようにサンプルに添加した。

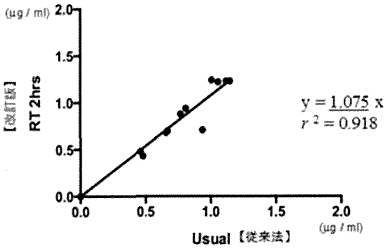

図5 可溶性CD26測定値の比較(従来法 v.s. 改訂版)

⇒ 可溶性CD26測定は、室温2時間の検体反応時間で
従来法と同等の測定結果が得られた。

可溶性CD26測定に関して、
検体反応時間は一晩から2時間まで短縮可能である。

3) DPPIV 酵素活性アッセイの性能試験と測定時間の簡便化

可溶性 CD26 同様に 4 種類の濃度の標準試料（10, 100, 300, 800ng/ml）を同時に 6 回測定することで同時再現性試験とした。表 3 に示したように 100ng/ml~800ng/ml では変動係数 CV が 10%以下と良好な結果を示した。しかし極低濃度（10ng/ml）では、ばらつきが大きかった。次に 4 種類の濃度の標準試料（10, 100, 300, 800ng/ml）を 5 回繰り返して測定することで測定間再現性試験とした。表 4 に示すように 100ng/ml ~ 800ng/ml では変動係数 CV が 10%以下と良好な結果を示した。しかし極低濃(10ng/ml)ではばらつきが大きかった。添加回収試験（Recovery）と直線性試験（Linearity）について添加回収試験（Recovery）は R&D system 社の Spike and Recovery Test protocol に従って実施した（図 4-1 参照）。「試料」は健常成人血清を 10 倍希釈したものを使用。「添加あり」は recombinant CD26 (R&D#1180-SE)を最終濃度 500ng/ml になるようにサンプルに添加した。Recovery は図 6 上段に示すように回収率 80~120%範囲内と良好な結果を示した。しかし「希釈なし」はやや不良であった。Linearity については図 6 下段に示すように添加なしの試料の直

線性は良好な結果を示した。添加ありの試料の直線性はやや不良であった。健常成人の血清検体を 4℃で保存して DPPIV 酵素活性を検討したところ 2 週間までは測定値の変化は認められなかった。次に健常成人の血清検体を 10 回まで凍結融解をくり返したが、測定値の変化は認められなかった。最後に DPPIV 酵素活性測定アッセイの測定時間の短縮化の検討を行った。従来の検体反応時間は一晩・静置・4℃で施行していたが 2 時間・穏やかに振盪、室温に変更して健常成人血清 11 例について DPPIV 酵素活性値を測定した。図 7 に示すように DPPIV 酵素活性は室温 2 時間の検体反応条件では低く測定されることが明らかになった。

表3 同時再現性試験(Intra-assay):
DPPIV酵素活性アッセイの性能試験

標準試料	テスト1	テスト2	テスト3	テスト4	テスト5	テスト6	Mean	SD	CV (%)
10 ng/ml	0.41	0.19	0.26	0.24	0.32	0.25	0.278	0.077	27.59
100 ng/ml	1.77	1.64	1.49	1.59	1.5	1.6	1.632	0.143	8.78
300 ng/ml	3.87	3.54	3.5	3.63	3.66	3.78	3.663	0.141	3.85
800 ng/ml	5.57	6.04	5.74	5.88	6.71	5.72	5.943	0.408	6.86

4種類の濃度の標準試料(10, 100, 300, 800ng/ml)を同時に6回測定することで同時再現性試験とした。DPPIV酵素活性値はμM/minで表示した。

⇒ 100ng/ml～800ng/mlでは変動係数CVが10%以下と良好な結果を示した。極低濃度(10ng/ml)ではバラつきが大きかった。

表4 測定間再現性試験(Inter-assay):
DPPIV酵素活性アッセイの性能試験

標準試料	プレート1	プレート2	プレート3	プレート4	プレート5	Mean	SD	CV (%)
10 ng/ml	0.28	0.33	0.24	0.23	0.30	0.27	0.04	14.69
100 ng/ml	1.63	1.99	1.86	1.77	1.82	1.81	0.13	7.17
300 ng/ml	3.66	3.68	3.37	3.36	3.89	3.59	0.23	6.31
800 ng/ml	5.94	5.53	5.76	6.25	5.82	5.86	0.26	4.50

4種類の濃度の標準試料(10, 100, 300, 800ng/ml)を5回繰り返して測定することで測定間再現性試験とした。DPPIV酵素活性値はμM/minで表示した。

⇒ 100ng/ml～800ng/mlでは変動係数CVが10%以下と良好な結果を示した。極低濃度(10ng/ml)ではバラつきが大きかった。

添加回収試験(Recovery)

	試料(添加あり)	試料(添加なし)	回収率(%)
希釈なし	5.49	1.26	78.18
1/2希釈	3.96	0.69	88.62
1/4希釈	2.30	0.29	90.99
1/8希釈	1.25	0.24	90.18

⇒回収率80～120%範囲内と良好な結果を示した。
「希釈なし」はやや不良であった。

直線性試験(Linearity)

		直線性(%)
試料(添加あり)	1/2希釈	119.88
	1/4希釈	128.55
	1/8希釈	134.06
試料(添加なし)	1/2希釈	108.61
	1/4希釈	117.84
	1/8希釈	118.12

⇒添加なしの試料の直線性は良好な結果を示した。
添加ありの試料の直線性はやや不良であった。

図6 添加回収試験(Recovery)と直線性試験(Linearity)

添加回収試験(recovery)はR&D Systems社のSpike and Recovery Test Protocolに従って実施した。「試料」は健常成人血清(を10倍希釈したもの)を使用。
「添加あり」はrecombinant CD26を最終濃度500ng/mLになるようにサンプルに添加した。

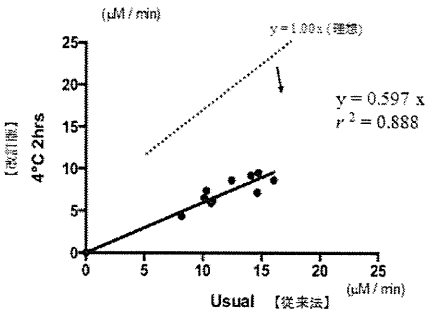

図7 DPPIV活性測定値の比較(従来法 v.s. 改訂版)

⇒ DPPIV活性測定は、2時間の検体反応時間では、低く測定される

DPPIV活性測定系では、検体希釈による
マトリックス効果の影響も考慮する必要あり

D. 考察

現在、糖尿病治療薬として DPPIV 酵素阻害薬が登場し、幅広く臨床現場に用いられている。

ヒト化 CD26 抗体を投与すると、血清中に存在する sCD26 と反応し、投与患者では sCD26 値及び DPPIV 酵素値が減少することが予想されることから sCD26 及び DPPIV 酵素活性値を治療経過でモニターにしていくことは抗体療法が安全に施行されるためにも必須である。

今までに可溶性 CD26 測定系として異なるエピトープと反応する CD26 抗体、5F8 及び 1F7 を用いたサンドイッチ ELISA 法及び DPPIV 酵素測定法としては固相化した 5F8 に可溶性 CD26 を捕捉させ、Gly-Pro-pNA を加えて、DPPIV 活性を測定する方法を確立した。しかしヒト化 CD26 抗体と 1F7 は同一エピトープを認識する CD26 抗体であるため(5F8 は異なるエピトープ) ヒト化 CD26 抗体治療患者では血清中の sCD26 にヒト化抗体が結合するため従来の CD26 検出 ELISA 系の 1F7 では sCD26 への結合が競合するために sCD26 は測定できなかった。

更に市販の可溶性CD26測定ELISAキットにおいてもヒト化 CD26 抗体が存在すると測定不能であった。今まで我々の開発したCD26 抗体の中で 9C11 抗体が従来のELISAに用いていた 1F7, 5F8 及びヒト化CD26 抗体とは異なるエピトープと反応する抗体であることを同定し可溶性 CD26 検出ELISA系において1F7 biotinの代わりに9C11 biotinに置き換えて、正常人血清にヒト化 CD26 抗体を加えてアッセイを行ったところ競合することなく可溶性 CD26 の測定が可能であった。しかも 9C11 を用いた新規 ELISA は市販の R&D 社の ELISA キットよりも感度が高いことが明らかとなった。フランスでのヒト化 CD26 抗体の第 I 相臨床試験は平成 26 年 9 月に終了して、安全性の確認及び期待される効果を示唆するデータも得られた。その全ての抗体投与患者において血清中の可溶性 CD26 は測定可能であり、更に抗体投与量が増加するにつれて、可溶性 CD26 濃度は低下し、可溶性 CD26 値とDPPIV酵素活性値は相関して動くことからDPPIV 酵素値も低下してDPPIV 阻害剤が投与されている病態を呈する可能性があり、ヒト化 CD26 抗体投与例において糖尿病薬服用者については特に低血糖発作などに注意する必要性が示唆された。可溶性CD26 定量 ELISA アッセイシステムの性能試験の結果はとても良好であった。更に可溶性 CD26 測定は検体反応時間も従来の一晩から二時間に短縮できた。一方でDPPIV 酵素活性アッセイシステムでは血清中の可溶性CD26/DPPIV分子のキャプチャー性能は良好であったが、極低濃度ではその測定にばらつきがあったり、添加ありの試料の直線性はやや不良であることが観察された。またDPPIV 酵素活性測定法については可溶性CD26 測定 ELISA とは異なり検体反応時間を短縮するとDPPIV酵素活性は低く測定された。これはDPPIV 酵素活性測定の際に血清中に干渉因子が存在し、その為に測定結果に影響を及ぼす可能性が示唆された。またDPPIV 酵素活性アッセイシステムの手順簡便化のためには測定干渉因子を最小化する条件検討が必要なことが明らかになった。今後標準物質を用いて市販の液層測定系と対比して検討予定である。

E. 結論

従来の可溶性 CD26/DPPIV 測定 ELISA 系に用いていた 2 種の CD26 抗体及びヒト化 CD26 抗体とは異なるエピトープのCD26抗体 9C11 を用いることにより血清中にヒト化 CD26 抗体存在下でも可溶性CD26/DPPIV を測定できる新 ELISA 系を確立した。本 ELISA 系は従来の ELISA 系と同等の感度を示し、市販の ELISA キットよりも格段に感度は高かった。フランスのヒト化 CD26 抗体投与の第 I 相臨床試験患者血清においてもブロックされることなく可溶性CD26/DPPIV値は適切に測定することができた。可溶性 CD26 ELISA アッセイシステムの性能はとても良好で検体反応時間も短縮できることが明らかとなった。しかしDPPIV 酵素活性測定アッセイでは血清中に存在する干渉因子などの影響で希釈検体などで測定値に影響を与える可能性が示唆され、また検体反応時間の簡便化はそれらの干渉因子の存在などで現時点では難しいことが示唆された。

G. 研究発表

1. 論文発表

1) Ohnuma K, Hatano R, Aune TM, Otsuka H, Iwata S, Dang NH, Yamada T, Morimoto C. Regulation of pulmonary GVHD by IL-26+CD4 T lymphocytes through CD26/caveolin-1 interaction. J Immunol. 2015; in press.

2) Otsuki N, Iwata S, Yamada T, Hosono O, Dang NH, Hatano R, Ohnuma K, Morimoto C. Modulation of immunological responses and amelioration of collagen-induced arthritis by the novel roxithromycin derivative 5-I. Mod Rheumatol. 2015; in press.

3) Ohnuma K, Saito T, Hatano R, Hosono O, Iwata S, Dang NH, Ninomiya H, Morimoto C. Comparison of two commercial ELISAs against an in-house ELISA for measuring soluble CD26 in human serum. J Clin Lab Anal. 2015; in press

4) Hatano R, Ohnuma K, Otsuka H, Komiya E, Taki I, Iwata S, Dang NH, Okumura K, Morimoto C. CD26-mediated induction of EGR2 and IL-10 as potential regulatory mechanism for CD26 costimulatory pathway. J Immunol. 2015; 194:960-972

5) Fujimoto N, Ohnuma K, Aoe K, Hosono O, Yamada T, Kishimoto T, Morimoto C. Clinical significance of soluble CD26 in malignant pleural mesothelioma. PLoS One 2014; 9:e115647

6) Nishida H, Suzuki H, Madokoro H, Hayashi M, Morimoto C. Sakamoto M, Yamada T. Blockade of CD26 Signaling Inhibits Human Osteoclast Development. J Bone Miner Res. 2014; 29: 2439-2455

7) Komiya E, Ohnuma K,Yamazaki H, Hatano R, Iwata S, Okamoto T, Dang NH, Yamada T, Morimoto C. CD26-mediated regulation of periostin expression contributes to migration and invasion of malignant pleural mesothelioma cells. Biochem Biophys Res Commun. 2014; 4: 609-615

8) Yamamoto J, Ohnuma K, Hatano R, Okamoto T, Komiya E, Yamazaki H, Iwata S, Dang NH, Aoe K, Kishimoto T, Yamada T, Morimoto C. Regulation of somatostatin receptor 4-mediated cytostatic effects by CD26 in malignant pleural mesothelioma. Br J Cancer. 2014; 110: 2232-2245

9) Kwan JC, Liu Y, Ratnayake R, Hatano R, Kuribara A, Morimoto C, Ohnuma K, Paul VJ, Ye T, Luesch H. Grassypeptolides as Natural Inhibitors of Dipeptidyl Peptidase 8 and T-Cell Activation. Chembiochem. 2014; 15:799-804.

2. 学会発表

1) 大沼圭, 斉藤辰彦, 波多野良, 岩田哲史, 鈴木博史, 森本幾夫. DPP4 阻害剤の服用によって誘発される多関節症とそのバイオマーカー. 第 58 回日本リウマチ学会学術集会, 2014 年 4 月 24－26 日, 東京

2) 波多野良, 大沼圭, 岩田哲史, 石井智徳, 関川巖, 森本幾夫. IL-10 産生誘導による CD26 共刺激経路の negative feedback 機構の解析. 第 58 回日本リウマチ学会学術集会, 2014 年 4 月 24－26

日，東京

H. 知的財産権の出願・登録状況（予定を含む）

1. 特許取得

なし

2. 実用新案登録

なし

3. その他

【本研究の進捗による特許出願】

発明の名称：免疫抑制剤
発明者　：森本幾夫、大沼圭、波多野良
出願者　：順天堂大学
種　類　：特許権
番　号　：特願2014-199260
出願日　：2014年9月29日
出願国　：PCT加盟国
概　略　：CD26分子のリガントCav-Ig蛋白が慢性GVHD治療に有効であるという特許である。

Ⅲ.　研究成果の刊行に関する一覧表

＜研究成果の刊行に関する一覧表＞

【雑　誌】

発表者氏名	論文タイトル名	発表誌名	巻号	ページ	出版年
Ohnuma K, Hatano R, Aune TM, Otsuka H, Iwata S, Dang NH, Yamada T, Morimoto C.	Regulation of pulmonary GVHD by IL-26+CD4 T lymphocytes through CD26/caveolin-1 interaction.	J Immunol.			in press
Otsuki N, Iwata S, Yamada T, Hosono O, Dang NH, Hatano R, Ohnuma K, Morimoto C.	Modulation of immunological responses and amelioration of collagen-induced arthritis by the novel roxithromycin derivative 5-I.	Mod Rheumatol.			in press
Ohnuma K, Saito T, Hatano R, Hosono O, Iwata S, Dang NH, Ninomiya H, Morimoto C.	Comparison of two commercial ELISAs against an in-house ELISA for measuring soluble CD26 in human serum.	J Clin Lab Anal.			in press
Hatano R, Ohnuma K, Otsuka H, Komiya E, Taki I, Iwata S, Dang NH, Okumura K, Morimoto C.	CD26-mediated induction of EGR2 and IL-10 as potential regulatory mechanism for CD26 costimulatory pathway.	J Immunol.	194	960-972	2015
Fujimoto N, Ohnuma K, Aoe K, Hosono O, Yamada T, Kishimoto T, Morimoto C.	Clinical significance of soluble CD26 in malignant pleural mesothelioma.	PLoS One	9	e115647	2014
Nishida H, Suzuki H, Madokoro H, Hayashi M, Morimoto C, Sakamoto M, Yamada T.	Blockade of CD26 Signaling Inhibits Human Osteoclast Development.	J Bone Miner Res.	29	2439-2255	2014
Komiya E, Ohnuma K,Yamazaki H, Hatano R, Iwata S, Okamoto T, Dang NH, Yamada T, Morimoto C.	CD26-mediated regulation of periostin expression contributes to migration and invasion of malignant pleural mesothelioma cells.	Biochem Biophys Res Commun.	4	609-615	2014

Yamamoto J, Ohnuma K, Hatano R, Okamoto T, Komiya E, Yamazaki H, Iwata S, Dang NH, Aoe K, Kishimoto T, Yamada T, Morimoto C.	Regulation of somatostatin receptor 4-mediated cytostatic effects by CD26 in malignant pleural mesothelioma.	Br J Cancer.	110	2232-2245	2014
Kwan JC, Liu Y, Ratnayake R, Hatano R, Kuribara A, Morimoto C, Ohnuma K, Paul VJ, Ye T, Luesch H.	Grassypeptolides as Natural Inhibitors of Dipeptidyl Peptidase 8 and T-Cell Activation.	Chembiochem.	15	799-804	2014
Fujimoto N, Kato K, Usami I, Sakai F, Tokuyama T, Hayashi S, Miyamoto K, Kishimoto T.	Asbestos-Related Diffuse Pleural Thickening.	Respiration	88	277-284	2014
Makimoto G, Fujiwara K, Fujimoto N, Yamadori I, Sato T, Kishimoto T.	Phrenic nerve paralysis as the Initial presentation in pleural sarcomatoid mesothelioma.	Case Rep Oncology	7	389-392	2014
藤本伸一、青江啓介、大泉聡史、上月稔幸、亀井敏昭、三浦溥太郎、井内康輝、岸本卓巳	胸膜中皮腫を中心とした胸水ヒアルロン酸に関する症例調査	肺癌	54(6)	767-771	2014
五十嵐毅、宇佐美郁治、岸本卓巳、水橋啓一、大西一男、大塚義紀、横山多佳子、藤本伸一、坂本浩一、中野郁夫、木村清延	じん肺症における血中アディポネクチンと炎症性マーカーについての検討	日本職業・災害医学会会誌	62(3)	184-188	2014
中野郁夫、岸本卓巳、宇佐美郁治、大西一男、水橋啓一、大塚義紀、五十嵐毅、藤本伸一、木村清延	じん肺における非結核性抗酸菌症の発生状況に関する研究	日本職業・災害医学会会誌	62(2)	117-122	2014

Ⅳ.　研究成果の別刷

CD26-Mediated Induction of EGR2 and IL-10 as Potential Regulatory Mechanism for CD26 Costimulatory Pathway

Ryo Hatano,*,† Kei Ohnuma,* Haruna Otsuka,* Eriko Komiya,* Izumi Taki,* Satoshi Iwata,* Nam H. Dang,‡ Ko Okumura,† and Chikao Morimoto*

CD26 is associated with T cell signal transduction processes as a costimulatory molecule, and CD26$^+$ T cells have been suggested to be involved in the pathophysiology of diverse autoimmune diseases. Although the cellular and molecular mechanisms involved in CD26-mediated T cell activation have been extensively evaluated by our group and others, potential negative feedback mechanisms to regulate CD26-mediated activation still remain to be elucidated. In the present study, we examine the expression of inhibitory molecules induced via CD26-mediated costimulation. We show that coengagement of CD3 and CD26 induces preferential production of IL-10 in human CD4$^+$ T cells, mediated through NFAT and Raf-MEK-ERK pathways. A high level of early growth response 2 (EGR2) is also induced following CD26 costimulation, possibly via NFAT and AP-1–mediated signaling, and knockdown of EGR2 leads to decreased IL-10 production. Furthermore, CD3/CD26-stimulated CD4$^+$ T cells clearly suppress proliferative activity and effector cytokine production of bystander T cells in an IL-10–dependent manner. Taken together, our data suggest that robust CD26 costimulatory signaling induces preferential expression of EGR2 and IL-10 as a potential mechanism for regulating CD26-mediated activation. *The Journal of Immunology*, **2015, 194: 960–972.**

CD26 is a 110-kDa type II membrane-bound glycoprotein with dipeptidyl peptidase IV (DPPIV) activity in its extracellular domain (1–3). CD26 is associated with T cell signal transduction processes as a costimulatory molecule, as well as being a marker of T cell activation (4, 5). Whereas CD26 expression is increased following activation of resting T cells, CD4$^+$ CD26^{high} T cells respond maximally to recall Ags such as tetanus toxoid (6). Moreover, crosslinking of CD26 and CD3 with solid-phase immobilized mAbs can induce T cell costimulation and IL-2 production by CD26$^+$ T cells. Furthermore, high CD26 cell surface expression in CD4$^+$ T cells is correlated with the production of Th1 and Th17-type cytokines and high migratory activity (4, 7). In fact, patients with autoimmune diseases, such as multiple sclerosis (MS), Grave's disease, and rheumatoid arthritis, have been found to have increased numbers of CD4$^+$CD26$^+$ T cells in inflamed tissues as well as in their peripheral blood, with enhancement of CD26 expression correlating with the autoimmune disease severity (8–10). We have recently found that cytotoxic activity of CD8$^+$ T cells is also regulated via CD26-mediated costimulation, and that CD26$^+$ T cells are deeply involved in the pathophysiology of acute graft-versus-host disease (11, 12). These findings imply that CD26$^+$ T cells play an important role in the inflammatory process and subsequent tissue damage in such diseases.

Activation of T cells through costimulatory signals is essential for an effective Ag-specific immune response, whereas the suppressive control of excessive immune responses is also critical for maintaining self tolerance and preventing autoimmunity. CD28 is a representative T cell costimulatory molecule, required for optimal production of cytokines and proliferation, and CD28-deficient mice have markedly reduced responses to exogenous Ags (13, 14). Alternatively, CTLA-4 functions as a potent negative regulator of the T cell response, and CTLA-4–deficient mice develop massive lymphadenopathy, autoimmunity, and early death (15, 16). Both CD28 and CTLA-4 are members of the Ig supergene family and are able to bind CD80 and CD86 expressed on APCs. CTLA-4 is not expressed on naive T cells, but it is induced after activation. CTLA-4 interacts with CD80 and CD86 with a 50- to 100-fold higher binding avidity than CD28, leading to interference of CD28 signaling (17). In addition to the ligand competition, the cytoplasmic domain of CTLA-4 associates with phosphatases SHP2 and PP2A to negatively regulate T cell activation, and it also inhibits the formation of lipid rafts (18). We have identified caveolin-1 on APCs as a functional ligand for CD26, and the ligation of CD26 with caveolin-1 recruits a complex consisting of CD26, CARMA1, Bcl10, MALT1, and IκB kinase to lipid rafts, leading to NF-κB activation (19, 20). CD26 possesses DPPIV enzyme activity, able to cleave dipeptides from polypeptides with N-terminal penultimate proline or alanine. Molecules displaying DPPIV-like enzymatic activity and/or structural similarity to the DPPIV/CD26 have been grouped to a family of "dipeptidyl pep-

*Department of Therapy Development and Innovation for Immune Disorders and Cancers, Graduate School of Medicine, Juntendo University, Tokyo 113-8421, Japan; †Atopy (Allergy) Research Center, Juntendo University Graduate School of Medicine, Tokyo 113-8421, Japan; and ‡Division of Hematology/Oncology, University of Florida, Gainesville, FL 32610

Received for publication August 28, 2014. Accepted for publication November 19, 2014.

This work was supported by a grant-in-aid from the Ministry of Education, Culture, Sports, Science and Technology, Japan (to K. Ohnuma and C.M.) and the Ministry of Health, Labor and Welfare, Japan (to C.M.), as well as Foundation of Strategic Research Projects in Private Universities Grant-in-Aid S1311011 from the Ministry of Education, Culture, Sports, Science and Technology, Japan (to C.M.). This work was also supported by Japan Society for the Promotion of Science KAKENHI Grant 26860760 (to R.H.) and Japan Society for the Promotion of Science Research Fellowships for Young Scientists (to R.H.).

Address correspondence and reprint requests to Dr. Chikao Morimoto, Department of Therapy Development and Innovation for Immune Disorders and Cancers, Graduate School of Medicine, Juntendo University, 2-1-1, Hongo, Bunkyo-ku, Tokyo 113-8421, Japan. E-mail address: morimoto@ims.u-tokyo.ac.jp

The online version of this article contains supplemental material.

Abbreviations used in this article: Cav-Ig, fusion protein of the N-terminal domain of human caveolin-1 and human IgG1 Fc; CD26 sup, supernatant of CD3/CD26-stimulated T cells; CD28 sup, supernatant of CD3/CD28-stimulated T cells; CyA, cyclosporin A; DPPIV, dipeptidyl peptidase IV; EGR2, early growth response 2; IRF4, IFN regulatory factor 4; LAG3, lymphocyte-activation gene 3; LAP, latency-associated protein; MFI, mean fluorescence intensity; MS, multiple sclerosis; siRNA, small interfering RNA; Treg, regulatory T cell; Tr1, type 1 regulatory T cell.

tidase IV activity and/or structure homologs (DASH)," including enzymatically active members such as fibroblast activation protein-α, quiescent cell proline dipeptidase/DPP-II/DPP7, DPP8, DPP9, and enzymatically inactive members such as DPP6 and DPP10 (21). However, a DASH family member that functions as a negative regulator of CD26-caveolin-1–mediated T cell activation has not yet been reported.

Active suppression by regulatory T cells (Tregs) is essential for the control of autoreactive cells. Tregs suppress immune responses through either direct cell–cell interactions or the release of inhibitory cytokines. $CD4^+CD25^{high}$ Tregs expressing FOXP3, a master regulatory gene for the suppressive activity, suppress immune cells mainly through soluble or membrane-bound TGF-β (22). Recently, IL-35 has been reported as a new inhibitory cytokine preferentially expressed by mouse $Foxp3^+$ Tregs, and it is required for their maximal suppressive activity (23). IL-35 is a member of the IL-12 heterodimeric cytokine family, composed of EBV-induced 3 and p35 (also known as IL-12α). Type 1 Tregs (Tr1s) are characterized by high-level production of IL-10 with regulatory activity (24). Lymphocyte-activation gene 3 (LAG3) and early growth response 2 (EGR2) have been recently reported as markers of Tr1-like cells (25). LAG3 binds to MHC class II molecules with higher affinity than CD4, leading to transduction of inhibitory signals for both T cells and APCs (26, 27). EGR2 is an essential transcription factor that regulates the T cell anergy program by directly upregulating diacylglycerol kinase α, and it also plays an important role in the induction of LAG3 and IL-10 expression (28).

Although the signaling events involved in CD26-mediated T cell activation or the cellular functions of CD26-expressing T cells have been studied extensively by our group and others, the potential negative feedback mechanism of CD26-mediated costimulation still remains to be elucidated. The present study focuses on the expression of inhibitory molecules induced in $CD4^+$ T cells following CD26 costimulation and the signaling pathways involved in this biological process.

Materials and Methods

Preparation of human T cells

Human PBMCs were collected from healthy adult volunteers after the documented informed consent and Institutional Review Board approval were obtained. This study has been performed according to the principles set out in the Declaration of Helsinki. For purification, the MACS cell separation system (Miltenyi Biotec, Bergisch Gladbach, Germany) and MACS human $CD4^+$ T cell isolation kit (Miltenyi Biotec) were used. Purity of $CD4^+$ T cells was ≥97% as confirmed by FACSCalibur (BD Biosciences, San Jose, CA).

Abs and reagents

For T cell stimulation, anti-CD3 mAb (OKT3), anti-CD28 mAb (4B10), anti-CD26 mAb (1F7), and the fusion protein of the N-terminal domain of human caveolin-1 and human IgG1 Fc (Cav-Ig) developed in our laboratory were used (20). The following human-specific Abs were used for flow cytometry: FITC-labeled anti-LAG3 mAb (clone 17B4) and FITC-labeled mouse IgG1, κ isotype control (clone MOPC-21) were purchased from Enzo Life Sciences (Farmingdale, NY). PE-labeled anti–CTLA-4 mAb (clone L3D10) and PE-labeled mouse IgG_1, κ isotype control (clone MOPC-21) were purchased from BioLegend (San Diego, CA). PE-labeled anti–IL-10 mAb (clone JES3-9D7) and PE-labeled rat IgG1, κ isotype control (clone eBRG1) were purchased from eBioscience (San Diego, CA). PerCP-labeled anti–latency-associated protein (LAP) mAb (clone 27232) and PerCP-labeled mouse IgG1 isotype control (clone 11711) were purchased from R&D Systems (Minneapolis, MN). Alexa Fluor 647–labeled anti–IFN-γ mAb (clone B27), Alexa Fluor 647–labeled anti-FOXP3 mAb (clone 259D/C7), and Alexa Fluor 647–labeled mouse IgG1, κ isotype control (clone MOPC-21) were purchased from BD Biosciences. Alexa Fluor 647–labeled anti-CD26 mAb (clone 19) recently developed in our laboratory was used for the detection of CD26 even in the presence of another anti-CD26 mAb, 1F7 (29). For Western blot analysis, mouse anti-NFAT1 mAb (clone 639402), goat anti-NFAT2 polyclonal Ab, and rabbit anti–p-ERK1 (pT202/pY204)/ERK2 (pT185/pY187) polyclonal Ab were purchased from R&D Systems. Mouse anti–TATA-binding protein mAb (clone mAbcam 51841) and rabbit anti-EGR2 mAb (clone EPR4004) were purchased from Abcam (Cambridge, U.K.). Mouse anti–β-actin mAb (clone AC-15) was purchased from Sigma-Aldrich (St. Louis, MO). HRP-conjugated sheep anti-mouse IgG and donkey anti-rabbit IgG were purchased from GE Healthcare (Buckinghamshire, U.K.), and HRP-conjugated donkey anti-goat IgG was purchased from Santa Cruz Biotechnology (Santa Cruz, CA). For neutralizing IL-10, anti–human IL-10 mAb (clone JES3-9D7), anti–human IL-10R mAb (clone 3F9), rat IgG1, κ isotype control (clone RTK2071), and rat IgG2a, κ isotype control (clone RTK2758) were purchased from BioLegend. Recombinant human IL-10 and the NFAT inhibitor cyclosporin A (CyA) were purchased from Sigma-Aldrich. The MEK1/2 inhibitor U0126 and the NF-κB activation inhibitor quinazoline were purchased from Merck Millipore (Billerica, MA).

Preparation of culture supernatant and measurement of cytokines

Purified $CD4^+$ T cells (1×10^5) were cultured in serum-free AIM-V medium (Invitrogen, Carlsbad, CA) in 96-well flat-bottom plates (Costar; Corning, Corning, NY), with stimulatory mAbs or Cav-Ig being bound in the wells beforehand at the following concentrations: 0.5 μg/ml OKT3 and/or 2, 5, 10, 20, or 50 μg/ml 4B10 or 1F7 or Cav-Ig. Cells were cultured in 5% CO_2 and 100% humidified incubator at 37°C for 48, 72, 96, or 120 h. After incubation, supernatants were collected and cytokine concentrations were examined using ELISA. BD OptEIA kits for human IL-2, IL-4, IL-5, IL-10, TNF-α, IFN-γ, or TGF-β1 were purchased from BD Biosciences, and the Ready-SET-Go! kits for human IL-17A or IL-21 were purchased from eBioscience. The absorbance at 450/570 nm was measured in a microplate reader (Bio-Rad, Hercules, CA), and data were analyzed with Microplate Manager 6 software (Bio-Rad).

Flow cytometry

Purified $CD4^+$ T cells (1×10^5) were incubated with plate-bound OKT3 (0.5 μg/ml) and/or 2, 5, 10, 20, or 50 μg/ml of 4B10 or 1F7 in 96-well flat bottom plates for 96 h, and cells were then collected and prepared for the analysis of cell surface expression of CTLA-4, LAG3, and LAP. Acquisition was performed using FACSCalibur, and data were analyzed with FlowJo software (Tree Star, Ashland, OR). For the analysis of intracellular FOXP3 and LAG3, a human FOXP3 buffer set (BD Biosciences) was used. For the staining of intracellular cytokines, cells were treated with GolgiStop (monensin) (BD Biosciences) for the last 5 h of culture in the presence or absence of 50 ng/ml PMA (Sigma-Aldrich) plus 1 μg/ml ionomycin (Merck Millipore) and then stained using BD Cytofix/Cytoperm Plus fixation/permeabilization kit (BD Biosciences) according to the manufacturer's instructions.

Preparation of lysates and Western blotting

To analyze nuclear expression of ERK or NFAT, purified $CD4^+$ T cells (1.5×10^6 cells/well, three wells per sample) were incubated with plate-bound OKT3 (0.5 μg/ml) and/or 4B10 (50 μg/ml) or 1F7 (50 μg/ml) in 24-well flat-bottom plates (Costar) for 0.5, 1, or 2 h. After incubation, cells were collected and nuclear extracts were prepared using EpiQuik nuclear extraction kit (Epigentek, Farmingdale, NY) supplemented with 2% protease inhibitor mixture (Sigma-Aldrich) and 1× PhosSTOP (Roche Diagnostics, Tokyo, Japan). For the analysis of EGR2 expression, purified $CD4^+$ T cells (1.5×10^6 cells/well) were stimulated in the above conditions for 24 or 48 h. After incubation, cells were collected and whole-cell lysates were prepared using RIPA buffer. Each sample was resolved by SDS-PAGE in reducing condition. SDS-PAGE and Western blot analysis were conducted as described previously (30). The images were taken using luminescent image analyzer LAS 4000 (GE Healthcare), and data were analyzed with image reader LAS 4000 and Multi Gauge software (GE Healthcare).

T cell proliferation assay

Purified $CD4^+$ T cells (1×10^5) were incubated with plate-bound OKT3 (0.5 μg/ml) and/or 4B10 or 1F7 in 96-well flat-bottom plates for 96 h in the presence or absence of signal inhibitor or culture supernatant. To evaluate T cell proliferation, a cell proliferation ELISA, BrdU Kit (Roche Diagnostics) was used. BrdU was added to each well for the last 2 h of incubation, and proliferation was assessed by measuring BrdU incorporation by ELISA. The absorbance at 450/655 nm was measured in a microplate reader, and data were analyzed with Microplate Manager 6 software. T cell proliferation was also assessed by using Cell Counting

Kit-8 (Dojindo, Kumamoto, Japan). 2-(2-Methoxy-4-nitrophenyl)-3-(4-nitrophenyl)-5-(2,4-disulfophenyl)-2H tetrazolium monosodium salt (WST-8) was added to each well at a concentration of 1/10 volume for the last 3 h, and the absorbance at 450/595 nm was measured. For the analysis of the number of cell divisions, a Vybrant CFDA SE cell tracer kit (Molecular Probes, Carlsbad, CA) was used. Purified $CD4^+$ T cells labeled with 2 μmol/l CFSE were incubated for 96 h with plate-bound stimulatory mAbs as described above, and cells were then harvested and analyzed by FACSCalibur.

Small interfering RNA against human EGR2

We selected two target sequences from nucleotides +1802 to 1820 (sense1) and +1890 to 1908 (sense2) downstream of the start codon of human EGR2 mRNA: sense1 small interfering RNA (siRNA), 5′-GAGUUGAUCUAAGACGUUUdTdT-3′, and sense2 siRNA, 5′-CACUUUAUGGCUUGGGACUdTdT-3′. siRNAs against EGR2 were purchased from Sigma-Aldrich, and negative control siRNA (oligonucleotide sequences are not disclosed) was purchased from Qiagen (Valencia, CA). Fifty picomoles siRNA duplexes were transfected into 5×10^5 purified $CD4^+$ T cells by using HVJ-E vector (GenomONE-Si; Ishihara Sangyo Kaisha, Osaka, Japan) according to the manufacturer's instructions (19, 20).

Quantitative real-time RT-PCR assay

Purified $CD4^+$ T cells or siRNA transfected $CD4^+$ T cells (5×10^5) were incubated with plate-bound OKT3 (0.5 μg/ml) and/or 4B10 or 1F7 or Cav-Ig in 24-well flat-bottom plates for 6, 12, 24, 48, or 72 h in the presence or absence of signal inhibitor or culture supernatant. After incubation, cells were collected and total RNA was extracted by the use of an RNeasy Micro kit according to the manufacturer's instructions (Qiagen). cDNA was produced by using a PrimeScript II first strand cDNA synthesis kit (TaKaRa Bio, Shiga, Japan) with oligo(dT) primers. Quantification of mRNA was performed using the 7500 real-time PCR System and SYBR Select Master Mix (Applied Biosystems, Foster City, CA). The obtained data were analyzed with 7500 System SDS software (Applied Biosystems), being normalized to hypoxanthine phosphoribosyltransferase expression. Sequences of primers used in quantitative real-time RT-PCR analysis are shown in Supplemental Table I.

Statistical analysis

Data were analyzed by the paired Student *t* test (two-tailed) for two group comparison, or by the ANOVA test for multiple comparison testing. The assay was performed in triplicate wells, and data are presented as mean ± SD of triplicate samples of the representative experiment, or mean ± SE of triplicate samples of independent experiments. Significance was analyzed using MS Excel (Microsoft) and p values < 0.01 were considered significant and are indicated in the corresponding figures and figure legends.

Results

CD26-mediated costimulation induces the development of $CD4^+$ T cells to a Tr1-like phenotype with high IL-10 production

To explore the negative feedback mechanism associated with CD26-mediated costimulation, we first examined the cytokine production profile of $CD4^+$ T cells, focusing particularly on the production of immunosuppressive cytokines such as TGF-β and IL-10. To characterize the specific phenotype associated with CD26 costimulation, we compared the level of cytokine production following costimulation with either CD26 or CD28, a representative T cell costimulatory pathway. As shown in Fig. 1A, only a small amount of cytokines was produced following stimulation with anti-CD3 mAb alone (gray lines), whereas both anti-CD3 plus anti-CD26 and anti-CD3 plus anti-CD28 costimulation greatly enhanced cytokine production (red or blue lines). Production of IL-10 by $CD4^+$ T cells was preferentially increased following CD26-mediated costimulation compared with CD28-mediated costimulation over the tested time intervals (Fig. 1Aa). IL-21 production was also greatly enhanced in the late phase of CD26 costimulation (Fig. 1Ab). Alternatively, production of IL-2, IL-5, or TNF-α was much lower following CD26 costimulation than CD28 costimulation (Fig. 1Af–h). In contrast, no difference in the production of IL-17A, IFN-γ, or IL-4 was observed following CD26- or CD28-mediated costimulation (Fig. 1Ac–e). Real-time RT-PCR analysis was then conducted to confirm the above results. As shown in Fig. 1B, IL-10 and IL-21 mRNA expression levels were higher after 24 h of CD26 costimulation than CD28 costimulation. Meanwhile, the amount of TGF-β1 was below the detection limit (0.125 ng/ml), and mRNA expression level of IL-35 subunits (EBV-induced 3 and p35) was not elevated following CD26- or CD28-mediated costimulation (data not shown). These data indicate that CD26 and CD28 costimulation of $CD4^+$ T cells results in different profiles of cytokine production, with IL-10 production being preferentially enhanced following CD26 costimulation.

To further characterize the biological process involved in IL-10 production following CD26 costimulation, we evaluated the effect of a wide range of concentrations of anti-CD26 and anti-CD28 mAbs. Additionally, to assess whether caveolin-1, a physiological ligand of CD26, can induce IL-10, we activated $CD4^+$ T cells with anti-CD3 mAb and Cav-Ig as described in *Materials and Methods*. As shown in Fig. 2Aa, CD26-mediated costimulation by both anti-CD3 plus anti-CD26 and anti-CD3 plus Cav-Ig greatly enhanced IL-10 production compared with CD28-mediated costimulation. It is noteworthy that the enhancement in CD26-mediated IL-10 production via either anti-CD26 mAb or Cav-Ig was dose-dependent, whereas IL-10 production decreased with increasing doses of anti-CD28 mAb (Fig. 2Aa). IL-17A production following CD26-mediated costimulation was similar to that observed following CD28-mediated costimulation (Fig. 2Ab). Although the amount of IL-2 produced by $CD4^+$ T cells following CD26 costimulation was 1–10 ng/ml and significantly higher than anti-CD3 mAb alone, it was consistently lower than that induced by CD28 costimulation (Fig. 2Ac, Supplemental Fig. 1A). T cell proliferation in response to CD26 costimulation was significantly decreased in the presence of neutralizing anti–IL-2 mAb, indicating that a relatively small amount of IL-2 induced by CD26 costimulation was sufficiently functional for enhancing T cell proliferation (Supplemental Fig. 1B). For further confirmation, we analyzed the intracellular expression of IL-10 in $CD4^+$ T cells through flow cytometry. Because inhibition of protein transport by monensin or brefeldin A is essential for intracellular cytokine staining, we analyzed IL-10 expression in T cells stimulated by anti-CD3 plus a high dose (50 μg/ml) of anti-CD26 or anti-CD28 with monensin for the last 5 h of culture. As shown in Fig. 2B, IL-10 and IFN-γ were equally induced in $CD4^+$ T cells following CD26 costimulation (Fig. 2Bb), whereas CD28 costimulation induced only IFN-γ but hardly induced IL-10 (Fig. 2Ba). Note that only ~2% of $CD4^+$ T cells expressed IL-10 following CD26 costimulation, but this induction was significant and was consistently seen in all the repeated experiments. In contrast with IFN-γ level, which was clearly detected by restimulation with PMA plus ionomycin, detection of the IL-10 level was relatively difficult because restimulation with PMA plus ionomycin hardly affected the percentage of IL-10–expressing cells following either CD26- or CD28-mediated costimulation (the results with similar stimulatory condition are shown in Fig. 6B). Previous work by Jonuleit et al. (31) investigating IL-10 expression also demonstrated a relatively low level of IL-10 expression when human peripheral blood $CD4^+$ T cells from healthy volunteers were primed and restimulated with allogeneic dendritic cells. We also noted that another anti-human IL-10 mAb from BD Biosciences gave similar results (data not shown). To define whether IL-10–expressing $CD4^+$ T cells following CD26-mediated costimulation expressed CD26, we stained cell surface CD26 and intracellular IL-10. For this purpose, as described in *Materials and Methods*, we used an anti-human CD26 mAb recognizing a different epitope from the one recognized by

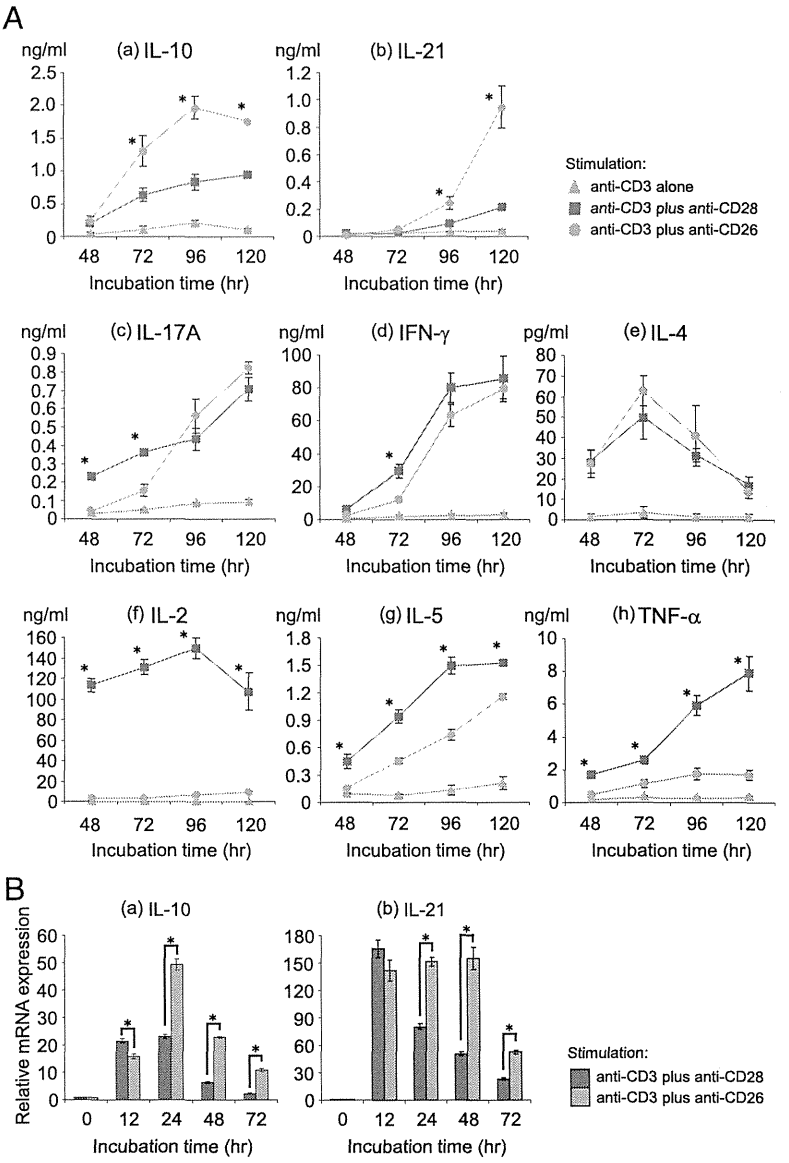

FIGURE 1. CD26-mediated costimulation of $CD4^+$ T cells induces greater levels of IL-10 and IL-21 than does CD28-mediated costimulation. Freshly purified $CD4^+$ T cells were stimulated with anti-CD3 mAb alone, anti-CD3 plus anti-CD28 mAbs (5 μg/ml), or anti-CD3 plus anti-CD26 mAbs (5 μg/ml) for the indicated times. (**A**) Concentrations of IL-10 (**a**), IL-21 (**b**), IL-17A (**c**), IFN-γ (**d**), IL-4 (**e**), IL-2 (**f**), IL-5 (**g**), and TNF-α (**h**) were examined by ELISA. (**B**) mRNA expression of IL-10 (**a**) and IL-21 (**b**) was quantified by real-time RT-PCR. Each expression was normalized to HPRT1, and relative expression levels compared with resting $CD4^+$ T cells (0 h) were shown. Representative data of seven (A) and three (B) independent donors are shown as mean ± SD of triplicate samples, comparing values in anti-CD3 plus anti-CD26 to those in anti-CD3 plus anti-CD28 ($*p < 0.01$), and similar results were obtained in each experiment.

the immobilized anti-CD26 mAb, 1F7, used for CD26 costimulation. As shown in Fig. 2Bc, all of the IL-10–expressing $CD4^+$ T cells were shown to express CD26. Taken together, these results indicate that CD26-mediated costimulation in $CD4^+CD26^+$ T cells preferentially induces IL-10, and this effect increases with enhancing intensity of CD26-mediated signaling.

We next examined the expression of selected molecules with well-characterized immunosuppressive functions by flow cytometry, including the cell surface expression of CTLA-4 and LAP complexed with TGF-β1, and the intracellular expression of transcription factor FOXP3. Because LAG3 has been reported to be continuously recycled and rapidly translocated to the plasma membrane in response to antigenic stimulation (32), we analyzed both the cell surface and intracellular expression of LAG3. As shown in Fig. 3, both the cell surface and intracellular expression of LAG3 was clearly enhanced with increasing doses of anti-CD26 mAb, and CD26-induced enhancement of LAG3 was more pronounced than the effect of CD28-mediated costimulation (Fig. 3Aa). Alternatively, both CD26- and CD28-mediated costimulation enhanced the expression of CTLA-4 and FOXP3, with no significant difference being detected between these two costimulatory pathways (Fig. 3Ac, d). In contrast with CD28 costimulation, LAP was hardly induced following CD26 costimulation (Fig. 3Ab). Although the mean fluorescence intensity (MFI) results of LAP, CTLA-4, or FOXP3 correlated with those of percentage of cells expressing LAP, CTLA-4, or FOXP3 shown in Fig. 3A, the values of MFI, especially for LAP and FOXP3, were low and the difference between CD26- and CD28-mediated costimulation was minimal (data not shown). Alternatively, as shown in Fig. 3B, all of the $CD4^+$ T cells expressed LAG3 following CD26 or CD28 costimulation, and no difference was observed in the percentage of LAG3-expressing cells, whereas the expression intensity of LAG3 after CD26-mediated costimulation was higher than after CD28-mediated costimulation. LAG3 also serves as a marker of IL-10–producing Tregs (25), suggesting that signaling events via CD26 may induce the development of $CD4^+$ T cells to a Tr1-like phenotype.

NFAT and Raf-MEK-ERK signalings are indispensable for CD26-mediated T cell activation

We next examined the signaling events associated with CD26-mediated enhancement in IL-10 production in $CD4^+$ T cells. Although cytokine receptor signaling through JAK-STAT plays a crucial role in T cell differentiation into specific effector subsets or Tregs, the initial signaling events for inducing cytokine production in T cells are associated with the TCR signaling pathway. Therefore, we first examined the effect of signal inhibitors against

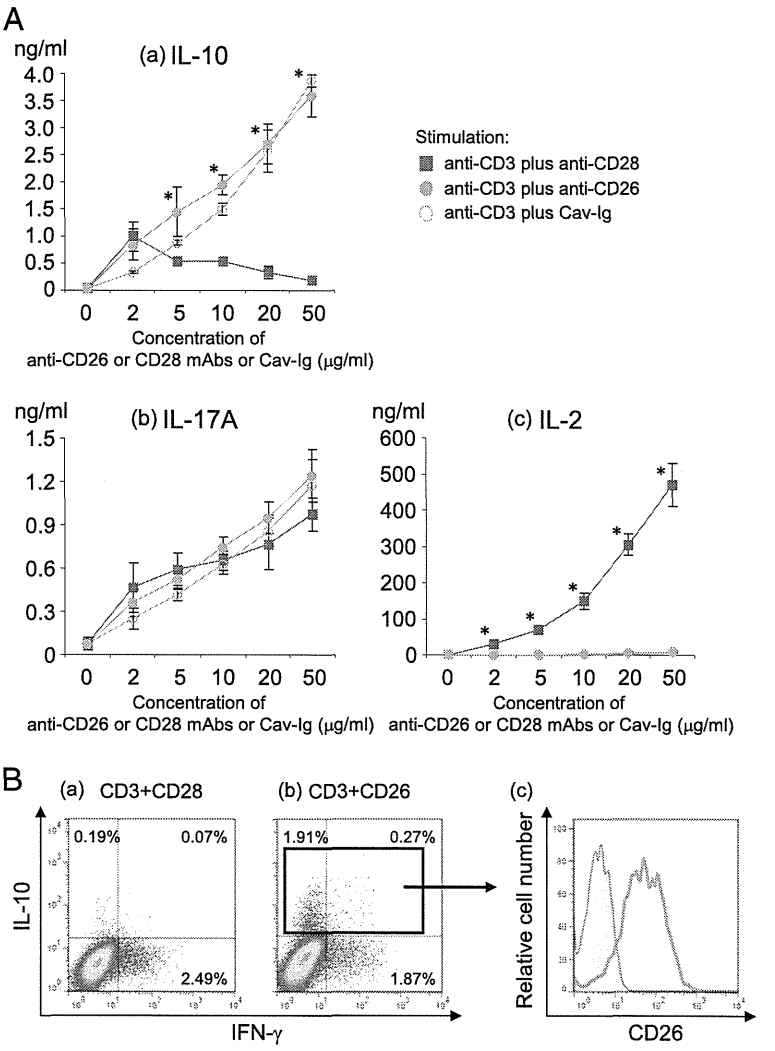

FIGURE 2. CD26-mediated costimulation of $CD4^+$ T cells greatly enhances IL-10 in a stimulation intensity–dependent manner. (**A**) Freshly purified $CD4^+$ T cells were stimulated with anti-CD3 mAb alone, anti-CD3 plus anti-CD28 mAbs, anti-CD3 plus anti-CD26 mAbs, or anti-CD3 mAb plus Cav-Ig at the indicated concentrations for 96 h. Concentrations of IL-10 (A**a**), IL-17A (A**b**), and IL-2 (A**c**) were examined by ELISA. Representative data of five independent donors are shown as mean ± SD of triplicate samples, comparing values in anti-CD3 plus anti-CD26 or anti-CD3 plus Cav-Ig to those in anti-CD3 plus anti-CD28 ($*p < 0.01$), and similar results were obtained in each experiment. (**B**) Freshly purified $CD4^+$ T cells were stimulated with anti-CD3 plus anti-CD28 mAbs (50 μg/ml) (**a**) or anti-CD3 plus anti-CD26 mAbs (50 μg/ml) (**b** and **c**) for 72 h. Cells were treated with monensin in the absence of PMA plus ionomycin restimulation for the last 5 h of culture, and cell surface CD26, intracellular IFN-γ, and IL-10 were detected by flow cytometry. (Ba and b) Two-dimensional dot plot of IFN-γ or IL-10 staining gated for $CD4^+$ T cells is shown. (Bc) Following gating for $CD4^+IL\text{-}10^+$ population as indicated in (Bb), the expression of CD26 was analyzed. The data are shown as histogram of CD26 intensity, and the gray area in the histogram show the data on the isotype control. A representative plot or histogram of four independent donors is shown, and similar results were obtained in each experiment.

NFAT, AP-1, or NF-κB, essential transcription factors for T cell activation located at the terminal end of TCR signaling. We first assessed T cell proliferation by measuring BrdU incorporation by ELISA, which is generally accepted to be equivalent to the [^{3}H]thymidine incorporation assay. As shown in Fig. 4A, the NFAT inhibitor CyA and the MEK1/2 inhibitor U0126 markedly inhibited the proliferative activity of $CD4^+$ T cells following CD26 or CD28 costimulation. Of note, T cells activated with anti-CD3 and anti-CD26 were much more sensitive to these inhibitors as compared with CD28 costimulation, and a high dose of CyA and U0126 suppressed the proliferation of T cells to the same level of proliferative activity as anti-CD3 alone (Fig. 4A). Additionally, we conducted a T cell proliferation assay by using tetrazolium salt, and results similar to those obtained with the BrdU incorporation assay were observed (Fig. 4B). As shown in Fig. 4C, the effects of NFAT and MEK1/2 inhibitors on IL-10 production were very similar to those on T cell proliferation. Whereas the NF-κB inhibitor quinazoline also suppressed T cell proliferation and IL-10 production in a dose-dependent manner, its effect on $CD4^+$ T cells following CD26 costimulation was less apparent as compared with NFAT and MEK1/2 inhibitors (Fig. 4A–C). These three inhibitors had similar effects on IL-17A and IFN-γ production as they did with IL-10 production (data not shown). These results indicate that both NFAT- and Raf-MEK-ERK–related signals are indispensable for CD26-mediated T cell activation, and they suggest that the intensity or persistence of these two signal pathways in $CD4^+$ T cells are different between CD26 and CD28 costimulation.

To further define the difference between CD26- and CD28-mediated costimulatory signaling pathways, we next examined the amount of NFAT and p-ERK1/2 translocated to the nucleus of $CD4^+$ T cells following CD26 or CD28 costimulation. The NFAT family consists of five members (NFAT1–5), and only NFAT5 is regulated by osmotic stress, not by calcium–calcineurin signaling (33). Because NFAT3 is reported to be absent in T cells, we analyzed the expression of NFAT1, NFAT2, and NFAT4. As shown in Fig. 4D, stimulation with both anti-CD3 plus anti-CD28 and anti-CD3 plus anti-CD26 resulted in increased nuclear levels of p-ERK1/2 and NFAT2 compared with anti-CD3 alone. Nuclear levels of p-ERK1/2 peaked at 30 min and then gradually decreased following CD28-mediated costimulation, whereas accumulation of NFAT2 in the nucleus reached a maximum after 2 h of CD28 costimulation. Alternatively, CD26-mediated costimulation resulted in greater enhancement of nuclear level of NFAT2 compared with CD28 costimulation, whereas the maximum level of p-ERK1/2 following CD26-mediated costimulation was lower than that seen with CD28 costimulation, but the effect of CD26 costimulation on p-ERK1/2 persisted until 2 h after stimulation. In contrast, no difference in nuclear level of NFAT1 was observed following CD26 or CD28 costimulation. As shown in Fig. 4D, when each sample was immunoblotted with anti-NFAT2, two bands were detected in molecular mass regions at ~110,000 and

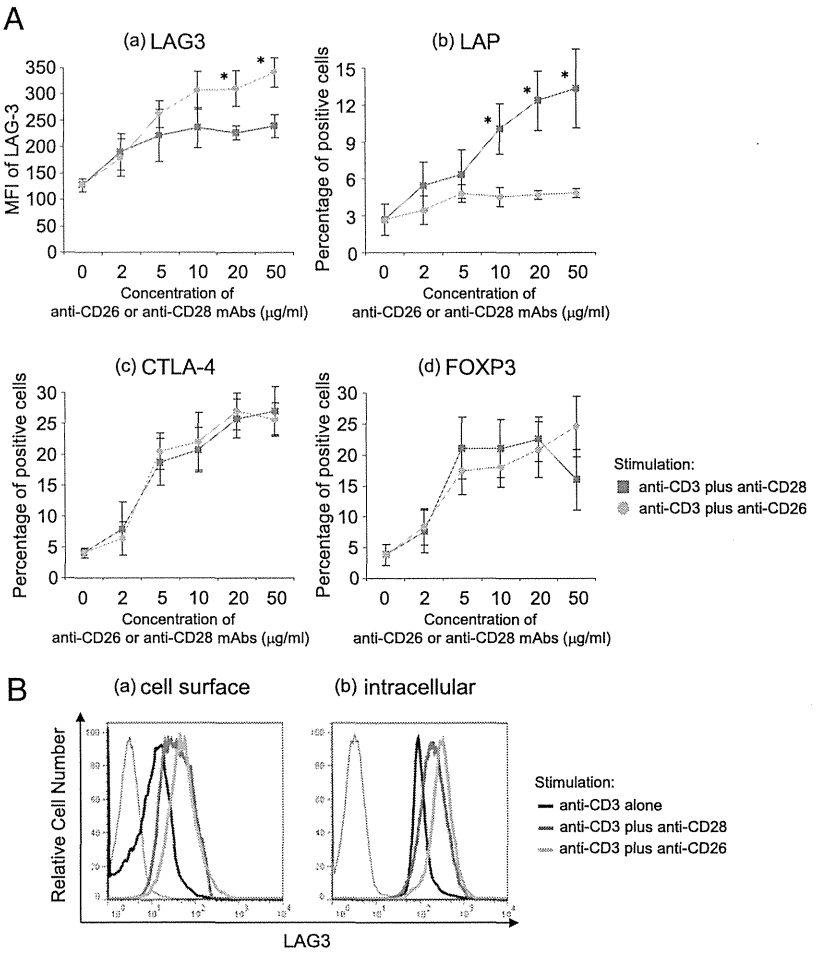

FIGURE 3. CD26-mediated costimulation of $CD4^+$ T cells induces greater LAG3 expression than does CD28-mediated costimulation. (**A**) Freshly purified $CD4^+$ T cells were stimulated with anti-CD3 mAb alone, anti-CD3 plus anti-CD28 mAbs, or anti-CD3 plus anti-CD26 mAbs at the indicated concentrations for 96 h. Cell surface LAP (A**b**), CTLA-4 (A**c**), intracellular LAG3 (A**a**), and FOXP3 (A**d**) gated for $CD4^+$ T cells were detected by flow cytometry. Data are shown as mean ± SE of MFI (Aa) or percentage positive cells (Ab–d) from five independent donors, comparing values in anti-CD3 plus anti-CD26 to those in anti-CD3 plus anti-CD28 (*$p < 0.01$), and similar results were obtained in each experiment. (**B**) Freshly purified $CD4^+$ T cells were stimulated with anti-CD3 mAb alone, anti-CD3 plus anti-CD28 mAbs (50 μg/ml), or anti-CD3 plus anti-CD26 mAbs (50 μg/ml) for 96 h. After stimulation, cell surface (a) or intracellular (b) expression of LAG3 gated for $CD4^+$ T cells was analyzed by flow cytometry. Data are shown as histogram of LAG3 and are representative of five independent donors. The gray areas in each histogram show the data of isotype control.

130,000 Da. The band with the higher molecular mass is thought to represent the constitutively expressed NFAT2 isoform, and the one with the lower molecular mass probably represents the inducible NFAT2 isoform (33). In contrast with NFAT4, which was only slightly expressed both in the cytoplasm and the nucleus of peripheral blood $CD4^+$ T cells (data not shown), the protein level of NFAT2 was abundant and clearly increased in response to CD26 or CD28 costimulation compared with NFAT1, suggesting that among the NFAT family, NFAT2 plays a crucial role in regulating human $CD4^+$ T cell activation. NFAT protein is known to synergistically interact with many transcription factors, including AP-1, which is the main transcriptional partner of NFAT during T cell activation. Alternatively, in the absence of AP-1, NFAT directs transcription of a specific program of gene expression that may be responsible for blocking TCR signaling (33). Taken together, these results strongly suggest that persistent NFAT–AP-1 cooperation is responsible for CD26-mediated T cell activation, leading to a specific pattern of gene expression different from CD28-mediated costimulation.

Increased EGR2 expression following CD26-mediated costimulation is associated with preferential IL-10 production

The findings above suggest that persistent NFAT–AP-1 activation following CD26-mediated costimulation is associated with enhanced IL-10 production. The molecular mechanisms involved in the process of IL-10 transcription in T cells have been well characterized, with the involvement of many transcription factors having been reported previously. c-Maf and IFN regulatory factor 4 (IRF4) directly transactivate IL-10 gene expression through binding to the IL-10 promoter (34, 35), whereas Blimp-1 positioned downstream of EGR2, GATA-3, and E4BP4 (also known as NFIL3) enhances IL-10 expression epigenetically by acetylating or methylating histones to change the chromatin structure at the IL-10 locus (36–38). We hypothesized that preferential IL-10 production of $CD4^+$ T cells following CD26-mediated costimulation was associated with the induction of such transcription factors. To validate the above assumption, we conducted a real-time RT-PCR assay to analyze the expression levels of the transcription factors discussed above following CD26 or CD28 costimulation. As shown in Fig. 5Aa, CD26 costimulation resulted in greater enhancement of EGR2 expression in $CD4^+$ T cells during the tested time intervals as compared with CD28 costimulation. Alternatively, both CD26 and CD28 costimulation markedly increased the expression of IRF4 compared with unstimulated T cells, but no difference was observed between these two costimulatory pathways (Fig. 5Ab). In contrast, both CD26 and CD28 costimulation of T cells led to a decrease in c-Maf or Blimp-1 expression (Fig. 5Ac, d), as well as a decline in expression levels of GATA-3 and E4BP4 (data not shown), indicating that EGR2 expression was preferentially induced following CD26-mediated costimulation. Western blot analysis was then conducted to confirm the above results. As shown in Fig. 5B, the protein level of EGR2 was higher after 24 or 48 h of CD26 costimulation than CD28 costimulation. Because it has been reported that EGR2 transcription is regulated by NFAT (39), we next examined the potential involvement of NFAT in the induction of EGR2 expression following CD26 costimulation. As shown in Fig. 5C, stimulation with both anti-CD3 plus anti-CD26 and anti-CD3 plus Cav-Ig clearly enhanced EGR2 expression compared with CD28 costimulation, a process that was partially inhibited by the NFAT

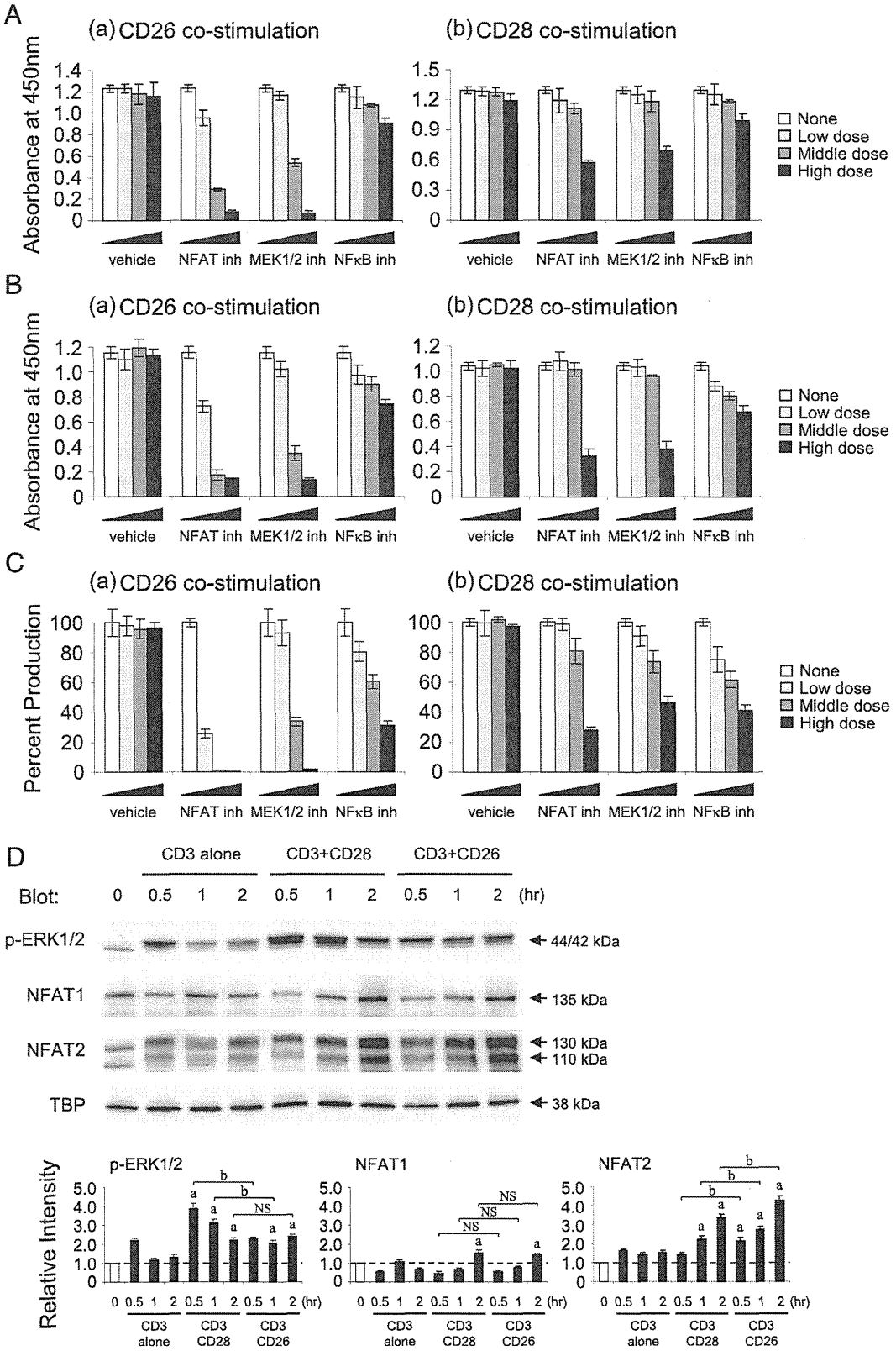

FIGURE 4. NFAT and Raf-MEK-ERK signaling events are indispensable for CD26-mediated CD4$^+$ T cell activation. (**A–C**) Freshly purified CD4$^+$ T cells were stimulated with anti-CD3 plus anti-CD26 mAbs (25 μg/ml) (**a**) or anti-CD3 plus anti-CD28 mAbs (25 μg/ml) (**b**) for 96 h in the presence of increasing doses of vehicle (DMSO, 0.0025, 0.0075, 0.025%), NFAT inhibitor (CyA, 0.01, 0.1, 1 μM), MEK1/2 inhibitor (U0126, 0.5, 1.5, 5 μM), or NF-κB inhibitor (quinazoline, 0.1, 0.5, 2.5 μM). (A) BrdU was added for the last 2 h of culture, and proliferation was assessed by measuring BrdU incorporation by ELISA. (B) Tetrazolium was added for the last 3 h of culture, and the absorbance at 450 nm was measured. (C) Concentration of IL-10 was examined by ELISA. Representative data of two (A) and four (B and C) independent donors are shown as mean ± SD of triplicate samples, and similar results were obtained in each experiment. (**D**) Freshly purified CD4$^+$ T cells were stimulated with anti-CD3 mAb alone, anti-CD3 plus anti-CD28 mAbs (50 μg/ml), or anti-CD3 plus anti-CD26 mAbs (50 μg/ml) for the indicated times. Nuclear extracts were separated by SDS-PAGE (each at 5 μg), and p-ERK1/2, NFAT1, or NFAT2 were detected by immunoblotting. The same blots were stripped and reprobed with Abs specific *(Figure legend continues)*

inhibitor alone and completely abrogated by the combination of the NFAT and MEK1/2 inhibitors. Furthermore, to determine whether EGR2 expression was associated with IL-10 production, we conducted knockdown experiments using siRNA against EGR2 in primary $CD4^+$ T cells. Expression level of EGR2 in T cells following CD26 costimulation was determined by real-time RT-PCR in the presence of control siRNA or two different sequences of EGR2-siRNA. As shown in Fig. 5Da, b, EGR2-siRNA treatment reduced EGR2 expression by ~50% as compared with control siRNA, which was associated with a significant decrease in IL-10 production by $CD4^+$ T cells. Because similar results were also obtained with a different siRNA sense2 designed to target a separate EGR2 site, data obtained with EGR2-siRNA sense1 as described in *Materials and Methods* are shown. Because it has been shown that EGR2-deficient $CD4^+$ T cells in mice produced high levels of IFN-γ and IL-17 following TCR stimulation (40), we therefore examined the effect of EGR2 knockdown on IL-17A and IFN-γ production by human $CD4^+$ T cells. As shown in Fig. 5Dc, d, production of both cytokines was vigorously enhanced by EGR2-siRNA compared with control siRNA. These results rule out the possibility that the decrease in IL-10 production seen with EGR2-siRNA treatment was due to the nonspecific off-target effects of siRNA. Taken together, these observations strongly suggest that CD26-mediated costimulation of $CD4^+$ T cells results in enhanced NFAT/AP-1–dependent EGR2 expression, which is associated with the preferential production of IL-10.

Supernatants of CD3/CD26-stimulated $CD4^+$ T cells suppress activation of bystander T cells in an IL-10–dependent manner

To address the functional significance of enhanced IL-10 production by $CD4^+$ T cells following CD26-mediated costimulation, we prepared culture supernatant of $CD4^+$ T cells stimulated with anti-CD3 plus a high dose (50 μg/ml) of anti-CD26 or anti-CD28 as a control and then examined whether the supernatant of CD3/CD26-stimulated T cells (CD26 sup) suppressed activation of bystander T cells. We confirmed that higher levels of IL-10 and lower levels of IL-2 were contained in CD26 sup as compared with the supernatant of CD3/CD28-stimulated T cells (CD28 sup), as shown in Fig. 2A. As shown in Fig. 6Aa, b, addition of CD26 sup to freshly purified $CD4^+$ T cells incubated under stimulatory condition with anti-CD3 plus anti-CD26 for 24 h resulted in a significant reduction in expression levels of both IL-2 and IFN-γ as compared with AIM-V medium, and this inhibitory effect was abrogated by the addition of anti–IL-10 plus anti–IL-10R. In contrast, IL-10 expression in $CD4^+$ T cells was significantly enhanced by CD26 sup, and this enhancing effect was almost completely reversed by anti–IL-10 plus anti–IL-10R (Fig. 6Ac). These results indicate that IL-10 contained in the CD26 sup suppresses the expression of effector cytokines such as IL-2 and IFN-γ but upregulated the expression of IL-10. Alternatively, treatment with CD28 sup markedly upregulated IL-2 expression, suggesting the presence in CD28 sup of soluble factors such as IL-2 that enhance the process of T cell activation (Fig. 6Aa). In contrast, addition of anti–IL-10 plus anti–IL-10R in the presence of CD28 sup increased the expression of IFN-γ but decreased IL-10 expression, suggesting that the relatively small amount of IL-10 in the CD28 sup was sufficient to regulate $CD4^+$ T cell cytokine production (Fig. 6Ab, c). To analyze the effect of CD26 sup on the proportion of IL-10 or effector cytokine-expressing cells, we next performed intracellular staining of IL-10 and IFN-γ in $CD4^+$ T cells. As shown in Fig. 6Ba, d, stimulation of freshly purified $CD4^+$ T cells with anti-CD3 plus anti-CD26 in the presence of CD26 sup for 3 d resulted in a decrease in the relative percentage of IFN-γ–expressing cells (from 18.5 to 11.1%) as compared with AIM-V medium, whereas the proportion of IL-10–expressing cells was hardly affected by CD26 sup. The effect of CD26 sup on the proportion of IFN-γ–expressing cells was reversed by anti–IL-10 plus anti–IL-10R (Fig. 6Be). Alternatively, addition of CD28 sup to $CD4^+$ T cells did not change the proportion of IFN-γ–expressing cells, but CD28 sup treatment in the presence of anti–IL-10 and anti–IL-10R led to an increase in the level of IFN-γ^+ cells (Fig. 6Bb, c), suggesting that the CD28 sup contained both activating and inhibitory factors such as IL-10. These findings strongly suggest that CD26 sup preferentially suppresses the proliferation of effector cytokine–expressing cells in an IL-10–dependent manner.

We next analyzed the effect of CD26 sup on T cell proliferation. As shown in Fig. 7A, CD26 sup clearly inhibited the proliferative activity of freshly purified $CD4^+$ T cells following CD26 costimulation. Although CD28 sup also slightly suppressed the proliferation of T cells following CD26 costimulation, the suppressive effect of CD26 sup was much more pronounced compared with CD28 sup. Interestingly, the suppressive effect on T cells following CD26 costimulation was more evident compared with T cells following CD28 costimulation (Fig. 7A). To further evaluate this observed difference, we conducted the same T cell proliferation assay in the presence of rIL-10. As shown in Supplemental Fig. 2A and 2B, T cells stimulated with anti-CD3 plus anti-CD26 were much more sensitive to the inhibitory effect of IL-10 as compared with CD28 costimulation, and the difference between CD26 and CD28 costimulation was markedly evident in cytokine production compared with proliferative activity. We further analyzed the expression of IL-10R on $CD4^+$ T cells following CD26- or CD28-mediated costimulation but observed no difference in the expression intensity of IL-10R between these two costimulatory approaches (Supplemental Fig. 2C). To characterize in more detail the effect of CD26 sup on T cell proliferation, we analyzed the cell division process of CFSE-labeled $CD4^+$ T cells by flow cytometry. As shown in Fig. 7Ba, b, d, e, CD26 sup exhibited a very potent suppressive effect on the proliferation of T cells stimulated with anti-CD3 plus anti-CD26 compared with CD28 sup, and this effect was partially reversed by addition of anti–IL-10 plus anti–IL-10R. It is noteworthy that 10 ng/ml rIL-10, a higher concentration than that found in CD26 sup, clearly suppressed T cell proliferation, but this effect was not more potent than CD26 sup (Fig. 7Bd, f). Alternatively, CD26 sup only slightly inhibited the proliferation of T cells stimulated with anti-CD3 plus anti-CD28, and these CD3/CD28-stimulated $CD4^+$ T cells were much less sensitive to the inhibitory effect of IL-10 as compared with CD3/CD26-stimulated T cells (Fig. 7Cc, d). These results correlated strongly with the proliferative activity shown in Fig. 7A. Taken together, these data strongly suggest that soluble factors secreted from $CD4^+$ T cells following CD26-mediated costimulation profoundly suppress bystander T cell proliferation, with IL-10 having a synergistic effect on the suppressive activity of these soluble factors.

for TATA-binding protein (TBP) as a loading control. Band intensity of p-ERK1/2, NFAT1, or NFAT2 was normalized to TBP, and relative intensity compared with resting $CD4^+$ T cells (0 h) is indicated in the *bottom panel*. Data are shown as mean ± SE of relative intensity from three independent donors, comparing values in anti-CD3 plus anti-CD28 or anti-CD3 plus anti-CD26 to those in anti-CD3 alone at the same stimulation period ($^a p < 0.01$), and anti-CD3 plus anti-CD26 to those in anti-CD3 plus anti-CD28 at the same stimulation period ($^b p < 0.01$).